Chaos, Solitons and Fractals 133 (2020) 109632

Contents lists available at ScienceDirect

Chaos, Solitons and Fractals

Nonlinear Science, and Nonequilibrium and Complex Phenomena

journal homepage: www.elsevier.com/locate/chaos

Fractional Lévy stable motion: Finite difference iterative forecasting model

He Liu[a], Wanqing Song[a,*], Ming Li[b,c], Aleksey Kudreyko[d], Enrico Zio[e]

[a] School of Electronic and Electrical Engineering, Shanghai University of Engineering Science, Shanghai 201620, PR China
[b] School of Information Science and Technology, East China Normal University, Shanghai 200241, PR China
[c] Ocean College, Zhejiang University, Hangzhou 316021, PR China
[d] Department of Medical Physics and Informatics, Bashkir State Medical University, Lenina st. 3, Ufa 450008, Russia
[e] Energy Department, Politecnico di Milano, Via La Masa 34/3, 20156, Italy

ARTICLE INFO

Article history:
Received 1 November 2019
Revised 11 January 2020
Accepted 14 January 2020

Keywords:
Fractional Lévy stable motion
Long-range dependence
Stochastic differential equation
Forecasting model

ABSTRACT

In this study we use the fractional Lévy stable motion (fLsm) to establish a finite iterative forecasting model with Long Range Dependent (LRD) characteristics. The LRD forecasting model considers the influence of current and past trends in stochastic sequences on future trends. We find that the discussed model can accurately forecast the trends of stochastic sequences. This fact enables us to introduce the fLsm as the fractional-order model of Lévy stable motion. Self-similarity and LRD characteristics of the flsm model is introduced by using the relationship between self-similar index and the characteristic index. Thus, the order Stochastic Differential Equation (FSDE) which describes the fLsm can be obtained. The parameters of the FSDE were estimated by using a novel characteristic function method. The forecasting model with the LRD characteristics was obtained by discretization of FSDE. The Monte Carlo method was applied to demonstrate the feasibility of the forecasting model. The power load forecasting history data demonstrates the advantages of our model.

1. Introduction

Forecasting of non-stationary stochastic sequences have been increasingly recognized in recent years. Many models have been developed to forecast the trend of such stochastic sequences as neural network [1], support vector machine [2], nonlinear forecasting models [3], fuzzy adaptive [4,5], etc. Since the mentioned models require a large number of training samples and other limitations, scholars have proposed to apply stchastic mathematical models to the field of stochastic sequence forecast,e.g., Gamma processes [6], Markov processes [7,8], and Wiener processes [9]. There are many slow change processes in engineering with stochastic and the LRD, and the characteristics of LRD are strong dependence at large intervals or lags. However, the existing stochastic models fail adequate reflect the interdependence of stochastic sequences (Fig. 1). In this article, we propose a fLsm-based stochastic forecasting model with LRD characteristics. The stochastic LRD model comprehensively considers the influence of the current and past states on the future states (Fig. 2), and dummyTXdummy-(can accurately forecast the trend of the stochastic sequence [10–13]. The fractional Brownian motion model with Gaussian and LRD characteristics is widely applied in this field [14–16]. In fact, stochastic sequences in practical applications have generally non-Gaussian properties [17]. Following practical situations, in this study we propose a forecasting model for stochastic sequences, which is based on fLsm with LRD and non-Gaussian characteristics [18].

Lévy motion (or Lévy process) is a stochastic process with stationary and independent increment, which is characterized by heavy-tailed distribution and infinite variance. The Lévy motion model can be applied to non-Gaussian distributions [19]. Such distributions as the Gaussian, Cauchy, and Poisson can obtained as particular cases of the Lévy motion [17]. In addition, the special cases for Lévy motion also include Lévy flights and Lévy walks [20–22]. When the incremental process of Lévy motion exhibit large jumps, the Lévy motion is called the Lévy flight. The length of these jumps is the subject of Lévy process with the power law tails. These jumps are also known as Lévy walks,which enhance the possibility to encounter sparsely distributed targets. The flexibility of Lévy motion modeling makes it universal for a broad range of stochastic problems [17,23,24]. In general, the corresponding definitions give different fractional Lévy motion if

* Corresponding author.
E-mail address: swqls@126.com (W. Song).

https://doi.org/10.1016/j.chaos.2020.109632
0960-0779/

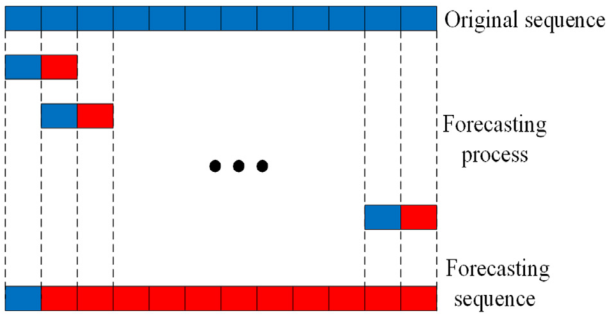

Fig. 1. Forecasting process of independent model.

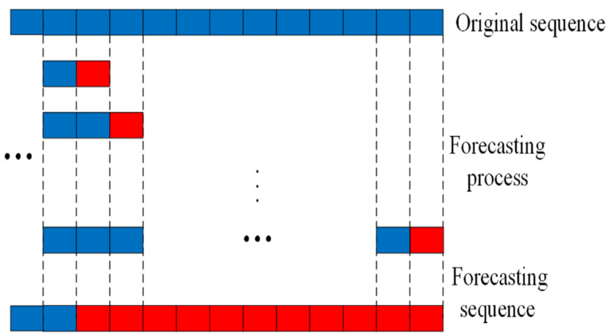

Fig. 2. Forecasting process of LRD model.

driving different Lévy motion [25,26], and refer to all different forms of fractional Lévy motion as the fractional Lévy motion group. Thus, more attention has been given to this issue. The fLsm driven by Lévy stable motion is mainly studied in this article.

The Lévy stable motion is described by parameters α, β, μ, δ [27] where the heavy-tailed degree of the probability density function is determined by the characteristic index α; the symmetry parameter β is used to describe how the skewed probability density function is spread around the centerline; μ indicates the location of a distribution; the dispersion degree is described by the scale parameter δ. We also note that the probability density function with the Lévy stable distribution does not have a closed expression, except for several exceptions. Therefore, the model characteristics are generally described by the characteristic function [28,29].

Earlier, Benassi et al. [30]introduced real-valued harmonic fractional Lévy processes, which are obtained by Lévy motion that have moments of every order. These processes have Holder paths and are locally asymptotically self-similar. Meanwhil, the moving-average fractional Lévy processes [31], which are thefields parameterized by a d-dimensional space, were introduced. These processes have Holder path and are locally self-similar. Non-anticipative fractional Lévy processes [32] are introduced by general Lévy motion with the zero mean, finite variance and without Brownian component, and they are not self-similar. As the fractional order model of Lévy motion, the fractional Lévy motion also describes the LRD characteristics [18] while describing the heavy-tailed distribution of stochastic processes, where LRD represents the relationship between the current value of a stochastic process and its historical values.

The fLsm is developed by Samorodnitsky et al. [14,18,33], and this model has explicit parameters for the stochastic differential equation, while other fractional Lévy motion models do not. The fLsm can be modified to other models if the characteristic index α changed, e.g., for $\alpha = 2$, the model transforms into fractional Brownian motion. Moreover, the LRD of fLsm is determined by the characteristic and self-similar indices α and H [28,34], respectively. For $\alpha H > 1$, the subsequent value of random sequence can be calculated from the previous sequence.

The fLsm can describe stochastic sequences with non-Gaussian and heavy-tailed properties, and can degenerate to fractional Brownian motion when the parameters of fLsm change [18], which can be modeled flexibly for random sequences. Application of fractional Brownian motion in stochastic sequences, which exhibiting LRD characteristics is a well-formed technique [15,35], but the fLsm rarely applies for forecasting of stochastic sequences. Hence, the finite iterative forecasting model with LRD characteristics based on the fLsm can be used forecasting for a wide range of stochastic sequences.

The fLsm can describe stochastic sequences with non-Gaussian and heavy-tailed properties, and can degenerate to fractional Brownian motion when the parameters of fLsm change [18], which can be modeled flexibly for random sequences. Application of the fractional Brownian motion for stochastic sequences,which exhibit LRD characteristics is a well-formed technique [15,35], but the fLsm rarely applies for forecasting of stochastic sequences. Hence, the finite iterative forecasting model with LRD characteristics based on the fLsm can be used forecasting for a wide range of stochastic sequences.

Since the fractional Lévy motion with LRD is not away a semimartingale processes [25,32], Itos formula cannot be applied. Fractional Itos formula [36–38] was applied to stochastic differential equation of Lévy stable motion [28] and the FSDE was obtained in this article. Then, the fractional Black–Scholes model [39,40] is extended and the parameterized FSDE is obtained. The fLsm is discretized by Taylor series expansion of fractional order [41] and substituted into the discrete FSDE. Finally, the expressions of the fLsm finite difference iterative forecasting model proposed was obtained by using discrete FSDE and difference equation.

Many mathematical methods, which deal with the probability density function are not applicable due to the lack of a closed form for the fLsm model [27]. The parameter estimation error is greatly influenced by the estimation method. Several parameter estimation methods were compared by in refs [27,29,42], where it is argued that the accuracy of the characteristic function method superiors other existing methods. Following this argument, we use the characteristic function method to estimate the parameters of FSDE [29].

This article is organized into five sections: The fLsm is introduced in Section 2, where we also analyze the model and LRD characteristics. The FSDE is proposed in Section 3, and the finite-difference iterative forecasting model is established by making the difference FSDE. The methodology of parameter estimation for the fractional order stochastic differential equation is given in the Appendix. The power load forecasting results show the feasibility of the finite-difference iterative forecasting model (Section 4). Some concluding remarks are given in Section 5.

2. Fractional Lévy stable motion: properties

A distribution is said to be stable whenever a linear combination of two independent random variables has the same distribution as the original distribution, which can be written as follows [17]:

$$x_1 + x_2 \cdots + x_n \triangleq ax + b.$$

here a and b are constants; x_i are independent and identically distributed random variables, and $\triangleq$ denote equality in distribution sense.

2.1. Characteristic of Lévy stable motion

The Lévy stable motion represents a non-Gaussian random process with LRD and high variability, which is often commonly

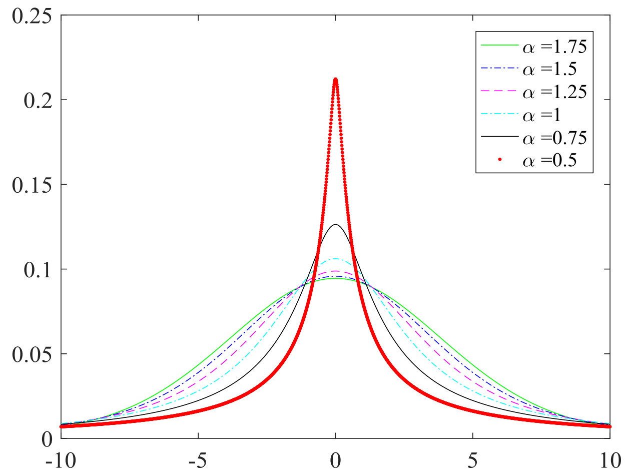

Fig. 3. Influence of different characteristic index values on the probability density function.

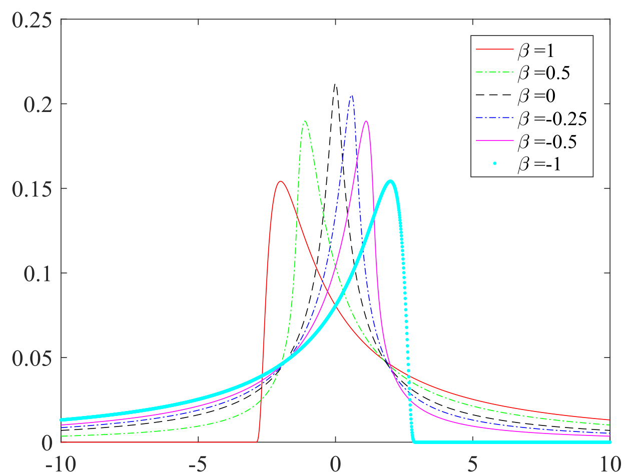

Fig. 4. Influence of different symmetry parameter values on the probability density function.

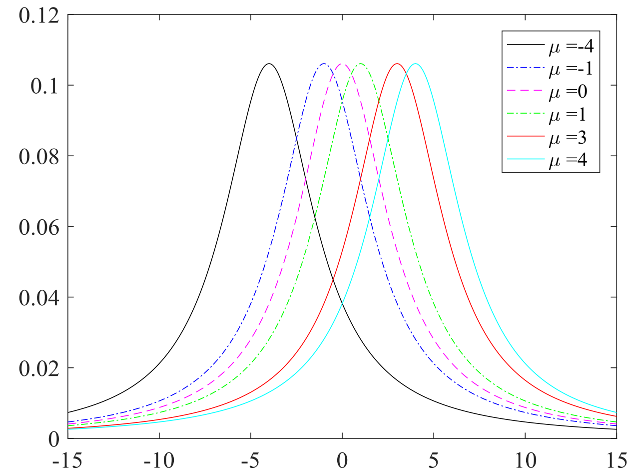

Fig. 5. The probability density function for different location parameter.

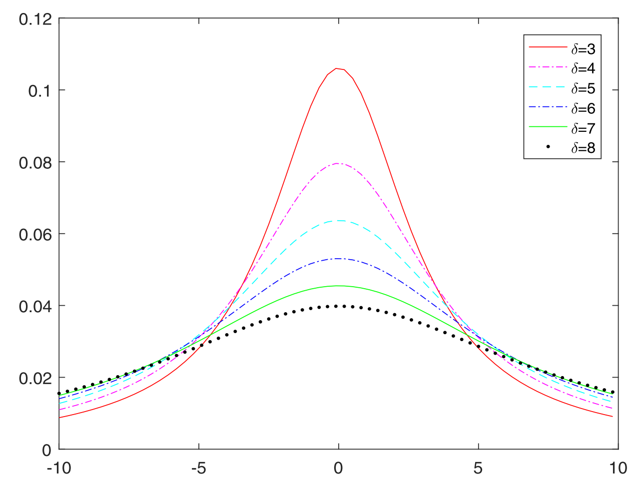

Fig. 6. The probability density function for different scale parameter.

encountered in natural processes. In the absence of a precise probability density function function [18,33]:

$$\varphi(\theta:\alpha,\beta,\delta,\mu)=E\left[e^{j\theta x}\right]=\begin{cases}\exp\left\{j\mu\theta-\delta|\theta|^{\alpha}\left[1-j\beta\frac{\theta}{|\theta|}\tan\left(\frac{\pi\alpha}{2}\right)\right]\right\}, \alpha\neq 1\\ \exp\left\{j\mu\theta-\delta|\theta|^{\alpha}\left[1+j\beta\frac{\theta}{|\theta|}\frac{2}{\pi}\ln|\theta|\right]\right\}, \alpha=1\end{cases}, \tag{1}$$

where the characteristic index α ranges within the interval:$0<\alpha\leq 2$. A clearer heavy tailed phenomenon of probability density function for different α is shown in Fig. 3. If we introduce parameter β ranging within the interval $-1\leq\beta\leq 1$, and denote it as the skewness index, then for $\beta>0$, the probability density function is right-skewed (and left-skewed for $\beta<0$). The symmetric stable distribution corresponds to $\beta=0$,(see Fig. 4); $\mu\in\mathbb{R}$ is the location parameter, which indicates the mean (Fig. 5). The spread parameter, $\delta>0$ represents the discrete nature of the distribution (Fig. 6).

2.2. Fractional Lévy stable motion model

The fLsm model is given by the following stochastic integral [17,18,43]:

$$L_{H,\alpha}(\mathrm{t})=\int_{-\infty}^{\infty}\left\{a\left[(t-s)_{+}^{H-1/\alpha}-(-s)_{+}^{H-1/\alpha}\right]\right.\\ \left.+b\left[(t-s)_{-}^{H-1/\alpha}-(-s)_{-}^{H-1/\alpha}\right]\right\}Mds, \tag{2}$$

where a and b are the arbitrary constants, $x_{+}^{H-1/\alpha}=0$ for $x\leq 0$ and $x_{+}^{H-1/\alpha}=x^{H-1/\alpha}$ for $x>0, M\in\mathbb{R}$ is the symmetric Lévy stable random measure, and H is the self-similarity parameter.

Similarly, we can also define the fLsm as the following Riemann-Liouville fractional integral [44]:

$$L_{H,\alpha}(t)=\frac{1}{\Gamma(H+1/2)}\int_{0}^{t}(t-\tau)^{H-1/2}dL_{\alpha}(\tau), \tag{3}$$

where $L_{\alpha}(\tau)$ is the symmetric Lévy stable distribution, $\Gamma(\cdot)$ is the gamma function. Fig. 7 shows the fLsm sequence generated with different α values for $H=0.75$. We observe that the random walk of the fLsm sequence increases as α increases.

2.3. Characteristic of fractional Lévy stable motion incremental processes

The incremental process for fLsm [i.e., the fractional Lévy stable noise is introduced by the fractional Gaussian noise] is derived by Samoradnitsky and Taqqu [17], Kogon and Manolakis [45]

$$\begin{aligned}b_H(t)&=B_H(t+1)-B_H(t)\\&=\int_{-\infty}^{\infty}\{a\left[(t+1-s)_{+}^{H-1/2}-(-s)_{+}^{H-1/2}\right]\\&\quad+b\left[(t+1-s)_{-}^{H-1/2}-(-s)_{-}^{H-1/2}\right]\}\omega(s)(ds),\end{aligned} \tag{4}$$

where $\omega(s)$ is the Gaussian white noise. Representation of fractional Lévy stable noise is acquired by transforming the exponent

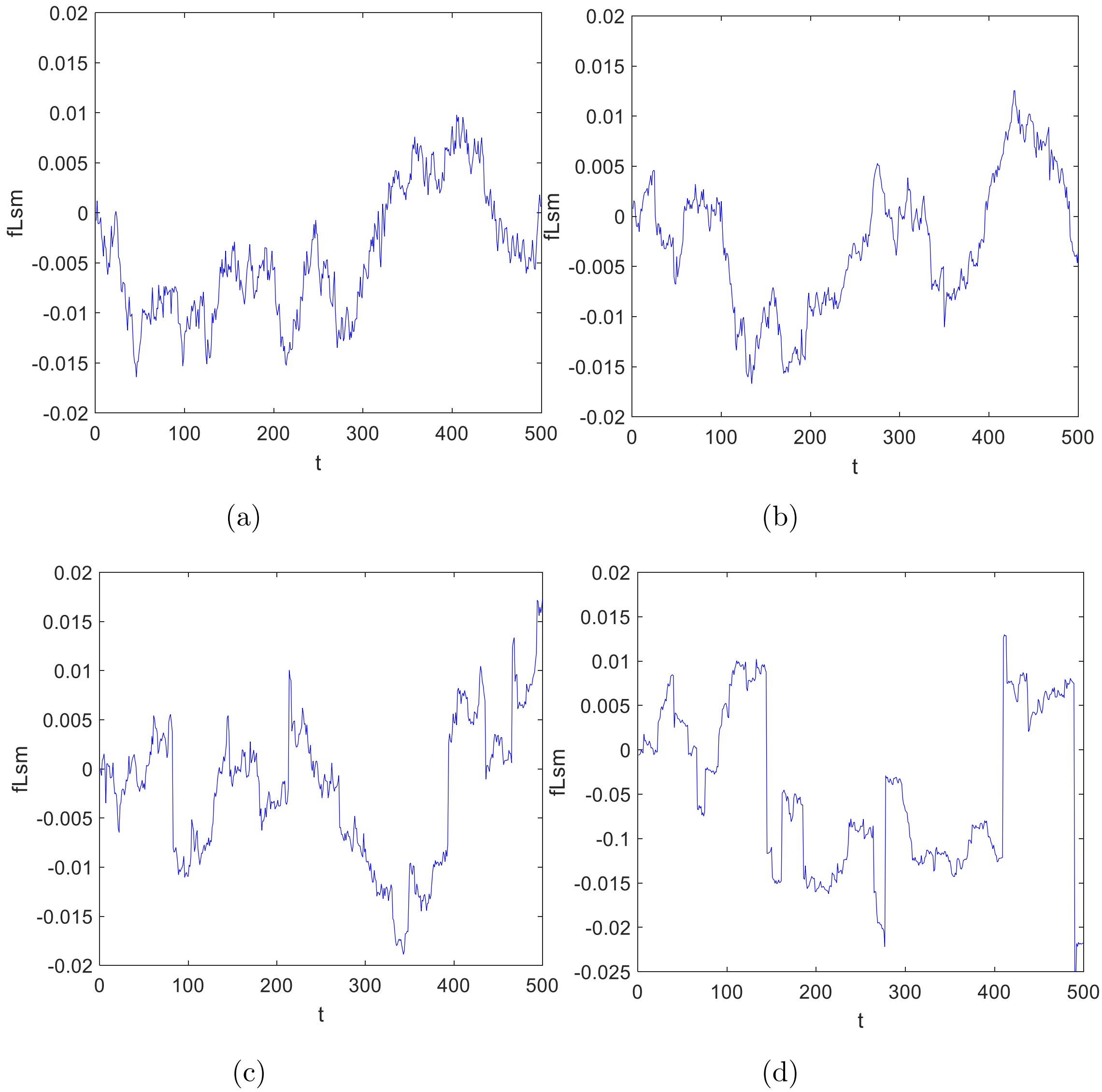

Fig. 7. FLsm generated with different $\alpha = 2, 1.75, 1.5, 1.25,$ respectively, $H = 0.75$.

in Eq. (4) from $H-1/2$ to $H{-}1/\alpha$, and a white noise generated Lévy stable motion replaces the Gaussian white noise as the driving function. The fractional Lévy stable noise is defined by:

$$\begin{aligned} l_{H,\alpha}(t) &= L_{H,\alpha}(t+1) - L_{H,\alpha}(t) \\ &= \int_{-\infty}^{\infty} \{a\big[(t+1-s)_+^{H-1/\alpha} - (-s)_+^{H-1/\alpha}\big] \\ &\quad + b\big[(t+1-s)_-^{H-1/\alpha} - (-s)_-^{H-1/\alpha}\big]\}\omega_\alpha(s)(ds), \end{aligned} \tag{5}$$

where $\omega_\alpha(s)$ is the Lévy stable white noise. Fig. 8 shows the fractional Lévy stable noise sequence generated with different α, where $H = 0.75$. We observe that the influence of noise increases as parameter α increases.

2.4. Long-range dependence and self-similarity of fractional Lévy stable motion

If the stochastic process satisfies the scale invariance, then it is a self-similar, and defined by the identity:

$$x(t) \triangleq a^{-H}x(at).$$

The methods, which are used to calculate self-similar parameters, include absolute value method, periodogram estimation method, wavelet estimation method, rescaled range method etc [15,46,47]. High accuracy is achieved if the rescaled range method is used [15]. Consequently, we use the rescaled range method for estimation of the self-similar parameters in LRD random process.

Symmetric Lévy stable motion is $1/\alpha$ self-similar, namely, $L_\alpha(t) \triangleq a^{-1/\alpha}L_\alpha(at)$ for all $a > 0$. Laskin et al. [44] proved that the fLsm is a self-similar process with self-similar parameter $H{-}1/2{+}1/\alpha$. The incremental process $\{L_{H,\alpha}(t_2)\text{-}L_{H,\alpha}(t_1)\}$ is also self-similar with $H{-}1/2{+}1/\alpha$.

The sequence has LRD characteristics for $H \in (1/2,\ 1)$ [12]. Hence, we limit parameter value H to the range (1/2, 1). We note that the fLsm model has no long memory when $0 < \alpha < 1$. $\alpha \in (1, 2)$ to ensure that it has the LRD characteristic [18]. The key feature of the fLsm model is that parameters α, H are not independent, since the fLsm has LRD condition for $\alpha H > 1$, i.e. $H > 1/\alpha$ [17,18].

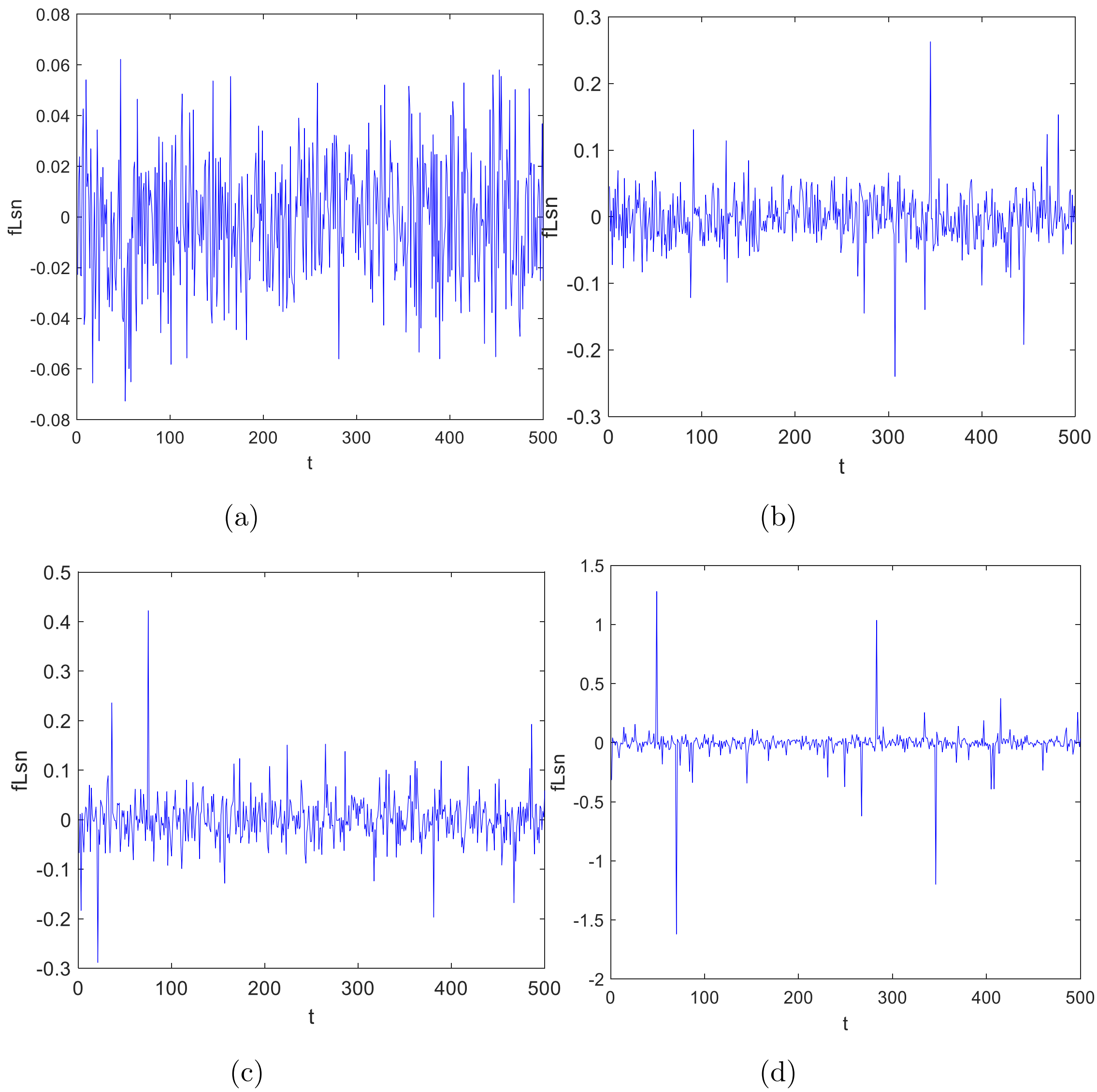

Fig. 8. Fractional Lévy stable noise generated with different $\alpha = 2, 1.75, 1.5, 1.25,$ respectively, $H = 0.75$.

3. Finite difference iterative forecasting model

3.1. Stochastic differential equation of fractional Lévy stable motion

The stochastic differential equation for Lévy stable motion was proposed by Janicki et al. [17,28,48], which reads as follows

$$dX(t) = a(t, X(t))dt + b(t, X(t))dL_\alpha(t) \qquad X(0) = X_0. \tag{6}$$

Eq. (6) can be represented in the integral form:

$$X(t) = X_0 + \int_0^t a(s, X(s-))ds + \int_0^t b(s, X(s-))\, dL_\alpha(s), \qquad t \geq 0. \tag{7}$$

In view of the fractional Ito's formula and derivation of stochastic differential equation for fractional Brownian motion [36–38,49], $L_\alpha(t)$ in Eq. (7) is replaced by $L_{H,\alpha}(t)$, and can be obtained the integral form of FSDE is obtained:

$$X_{H,\alpha}(t) = X_{(H,\alpha)_0} + \int_0^t a(s, X_{H,\alpha}(s-))ds + \int_0^t b(s, X_{H,\alpha}(s-))\, dL_{H,\alpha}(s), \qquad t \geq 0. \tag{8}$$

The differential form of Eq. (8) reads as follows:

$$\begin{aligned} dX_{H,\alpha}(t) &= a(t, X_{H,\alpha}(t))dt + b(t, X_{H,\alpha}(t))dL_{H,\alpha}(t) \\ X_{H,\alpha}(0) &= X_{(H,\alpha)_0}, \end{aligned} \tag{9}$$

where $a(t,\ X(t))$ and $b(t,\ X(t))$ represent drifting and diffusion functions, respectively.

The fractional Black–Scholes model [39,50],which was developed by Dai et al. [38,40,49,51] the following has expression:

$$dS_t = \mu S_t dt + \delta S_t dB_H(t), \tag{10}$$

where μ indicates the expected return rate, δ is the volatility rate. In fLsm, the model reduces to fractional Brownian motion when $\alpha = 2$ is used, μ represents the mean, and δ represents the diffusion coefficient; meanwhile, μ is the expected value and δ is the diffusion coefficient in $1 < \alpha \leq 2$, At this point, the drift and diffusion functions of the FSDE can be represented by $\mu X_{H,\alpha}(t)$ and $\delta X_{H,\alpha}(t)$, respectively. Consequently, Eq. (9) can be rewritten as follows:

$$dX(t) = \mu X(t)dt + \delta X(t)dL_{H,\alpha}(t), \tag{11}$$

where constants μ, δ are calculated from the novel characteristic function method,which is given in the Appendix.

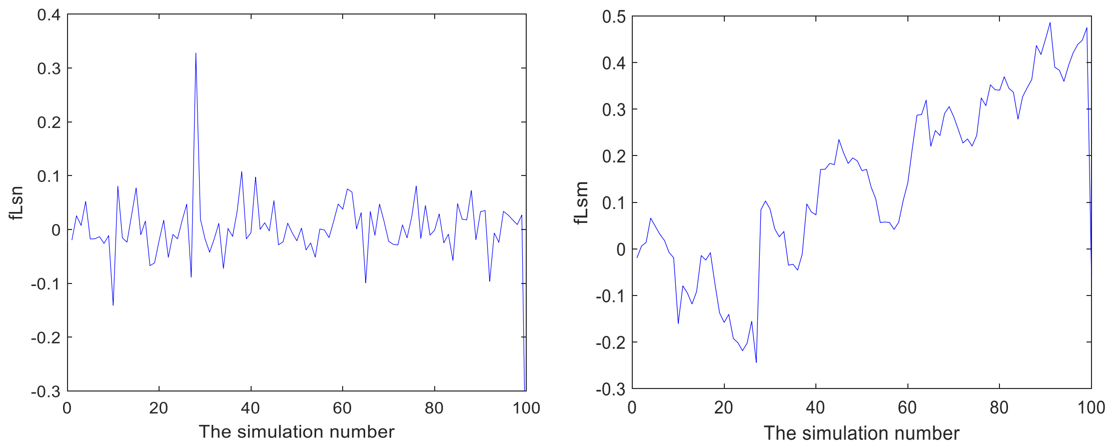

(a) The fractional Lévy stable noise simulation

(b) The fLsm simulation

Fig. 9. FLsm and fractional Lévy stable noise simulation series generated with $\Delta t = 0.01, H = 0.75, \alpha = 1.75$.

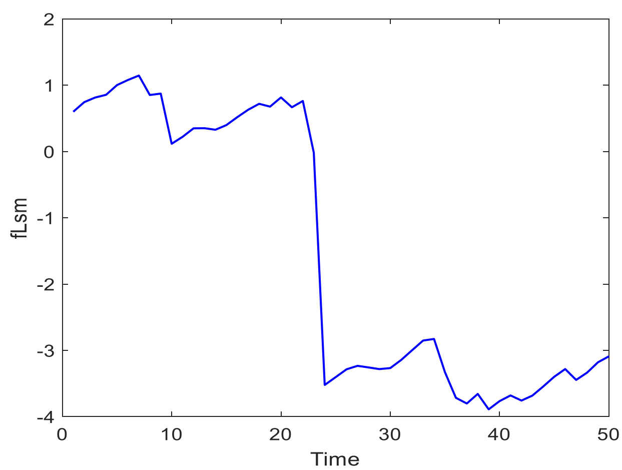

Fig. 10. FLsm sequences generated with $\alpha = 1.5, \beta = 0, \mu = 0.4586, \delta = 0.0396, H = 0.75, X_0 = 0.6$, by the Monte Carlo Simulation.

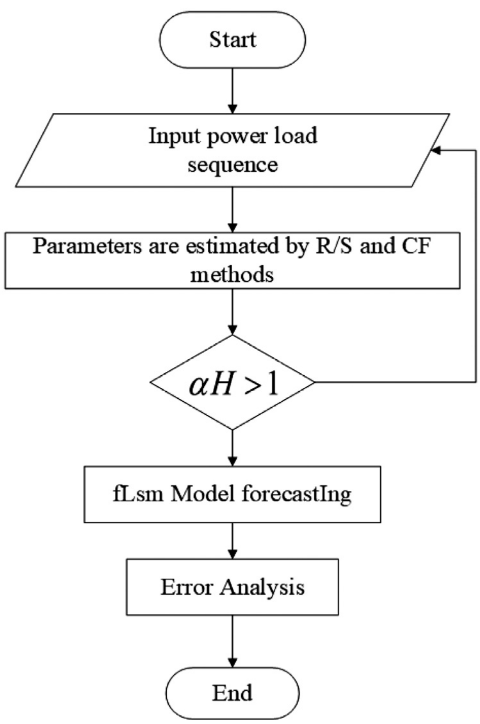

Fig. 11. Forecasting process.

3.2. Iterative forecasting model

By using the Maruyama notation [41] $dB_t = w(t)(dt)^{1/2}$, the following equations can be obtained:

$$\int_0^t f(\tau)(d\tau)^\rho = \rho\int_0^\tau (t-\tau)^{\rho-1} f(\tau)d\tau \quad , \tag{12}$$

$$dx = f(t)(dt)^\rho, \tag{13}$$

where $0 < \rho < 1$. The incremental expression of fLsm can be obtained by replacing $f(t)$ with $w_\alpha(t)$:

$$\int_0^t w_\alpha(\tau)(d\tau)^{H-\frac{1}{2}+\frac{1}{\alpha}} = \left(H-\frac{1}{2}-\frac{1}{\alpha}\right)\int_0^\tau (t-\tau)^{H-\frac{3}{2}+\frac{1}{\alpha}} w_\alpha(\tau)d\tau \quad , \tag{14}$$

$$dL_{H,\alpha} = w_\alpha(t)(dt)^{H-\frac{1}{2}+\frac{1}{\alpha}}. \tag{15}$$

The differential $dL_{H,\alpha}$ can be expressed as in the finite difference form:

$$\Delta L_{H,\alpha}(\Delta t, H) = L_{H,\alpha}(t+\Delta t, H) - L_{H,\alpha}(t, H) = w_\alpha(t)(\Delta t)^{H-\frac{1}{2}+\frac{1}{\alpha}}, \tag{16}$$

where the time interval [0, T] is sampled into N equal subintervals, in such a way that $\Delta t = T/N$. Let $T = 1, N = 100, \Delta t = 0.01, H = 0.75, \alpha = 1.75$.Then the simulated fLsm and the fractional Lévy stable noise can be plotted (see Fig. 9).

Eq. (11) can be written the discrete form, which reads as follows:

$$\Delta X_{H,\alpha}(t) = \mu X_{H,\alpha}(t)\Delta t + \delta X_{H,\alpha}(t) w_\alpha(t)(\Delta t)^{H-\frac{1}{2}-\frac{1}{\alpha}}, \tag{17}$$

The iterative forecasting model is obtained from the identity $\Delta X(t) = X(t+1) - X(t)$:

$$L_{H,\alpha}(t+1) = L_{H,\alpha}(t) + \mu L_{H,\alpha}(t)\Delta t + \delta L_{H,\alpha}(t) w_\alpha(t)(\Delta t)^{H-\frac{1}{2}-\frac{1}{\alpha}} \tag{18}$$

By using the Monte Carlo simulations [52], most likely curves for multiple time series can be generated. Supposing that

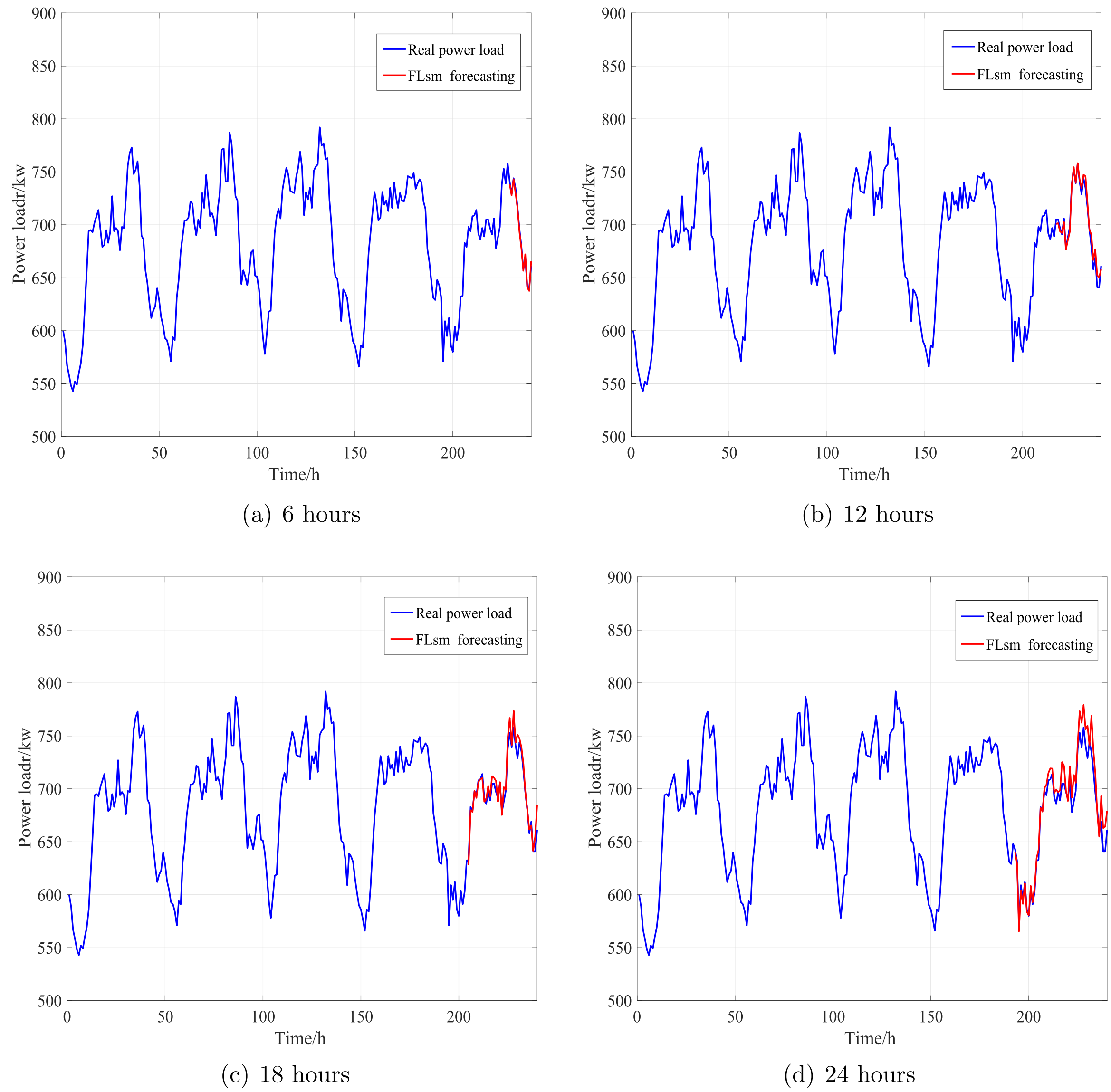

Fig. 12. Real 96-hour power load and the subsequent forecasted 24-hour trend plots.

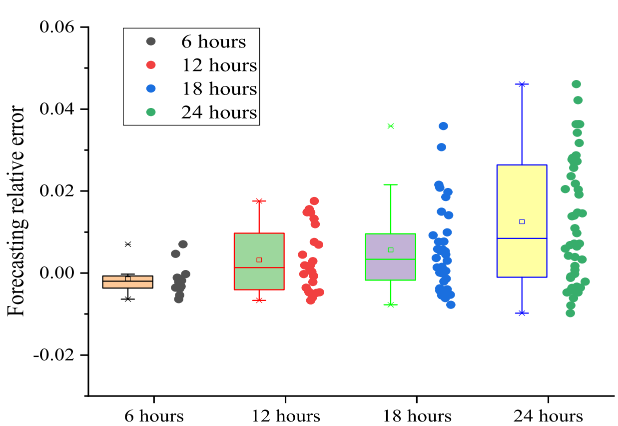

Fig. 13. Box plot analysis of relative error.

$\alpha = 1.5, \beta = 0, \mu = 0.4586, \delta = 0.0396, H = 0.75, X_0 = 0.6,$ and we simulate Monte Carlo 50 times. Fig. 10 shows the sequence simulated by the Monte Carlo method. It can be seen that the sequences generated by Eq. (18) are the same as the sequences generated by fLsm model.

4. Case studying

To verify the validity of the fLsm forecasting model, this experiment based on the fLsm forecasting model to forecasting the power load curve of the next 6, 12, 18 and 24 h for historical data. The real power load data is collected by Eastern Slovakian Electricity Corporation [53], which were sampled every 30 min. Three sets of historical power load data are used as sampling inputs, respectively, which use the R/S and the novel characteristic function method to calculate parameters (see Table 1). According

Table 1
Parameter estimation of forecasting model.

	H	α	μ	δ
Case 1	0.7464	1.7034	638.6514	4.0435
Case 2	0.7806	1.7104	548.8544	2.4709
Case 3	0.8644	1.6977	691.6931	2.7441

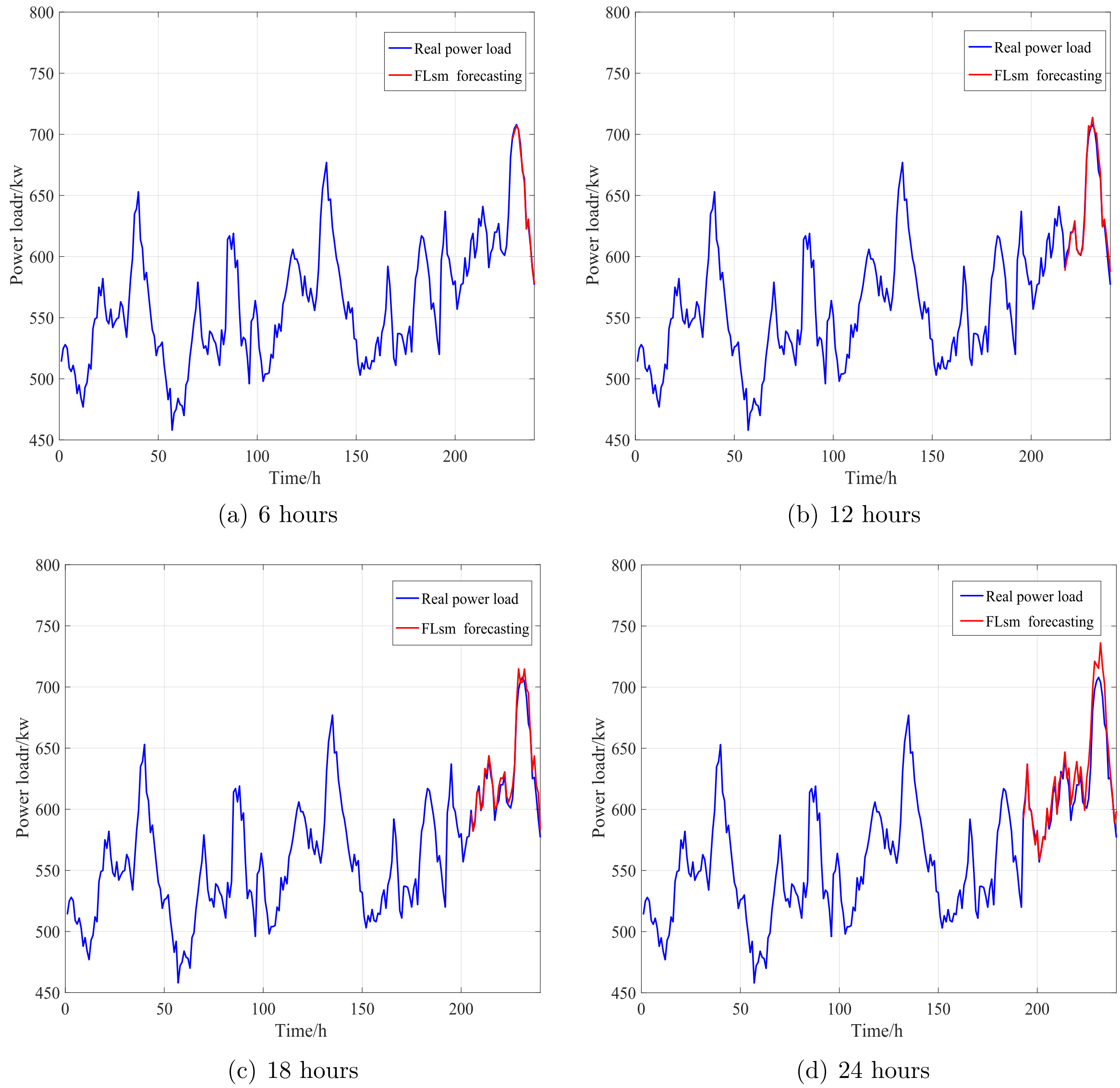

Fig. 14. Weekend power load forecasting trend.

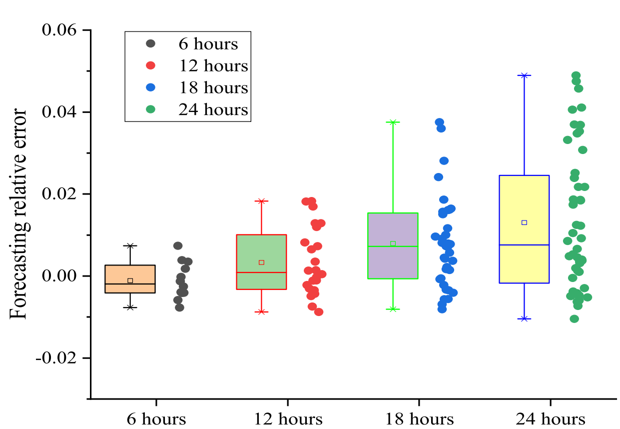

Fig. 15. Box plot analysis of relative error.

to the judgment condition $\alpha H > 1$, both sets of data have LRD characteristics. Therefore, the two sets of data are modeled by the fLsm forecast model, respectively. The experimental process of this article is shown in Fig. 11.

4.1. Case 1: Workday

To verify the power effect of the fLsm model, the power load of the fourth week of workday in October was used as input sequence.The power load of Monday to Thursday was used as historical data to forecast trend of power load on Friday. Since the electricity consumption on the workday is similar, and it is close to Friday from Monday to Thursday, it can accurately reflect trend of power load data. This parameter set were substituted into the iterative forecasting model. Trend of historical data set was forecasted for the subsequent 6, 12, 18 and 24 h with the MATLAB simulation. The 24-hour forecasting trend for historical data is shown in Fig. 12. Analysis of relative error of forecasting results, such as maximum, mean, median, stand deviation and mean absolute percentage error(MAPE) are shown in Table 2, and the box plot of the relative error is shown in Fig. 13, which shows the maximum value of the relative error clearly.

4.2. Case 2: Workday and weekend

We repeated the analysis of Case 1, but we used the weekend of the first two weeks of October to forecast the power load

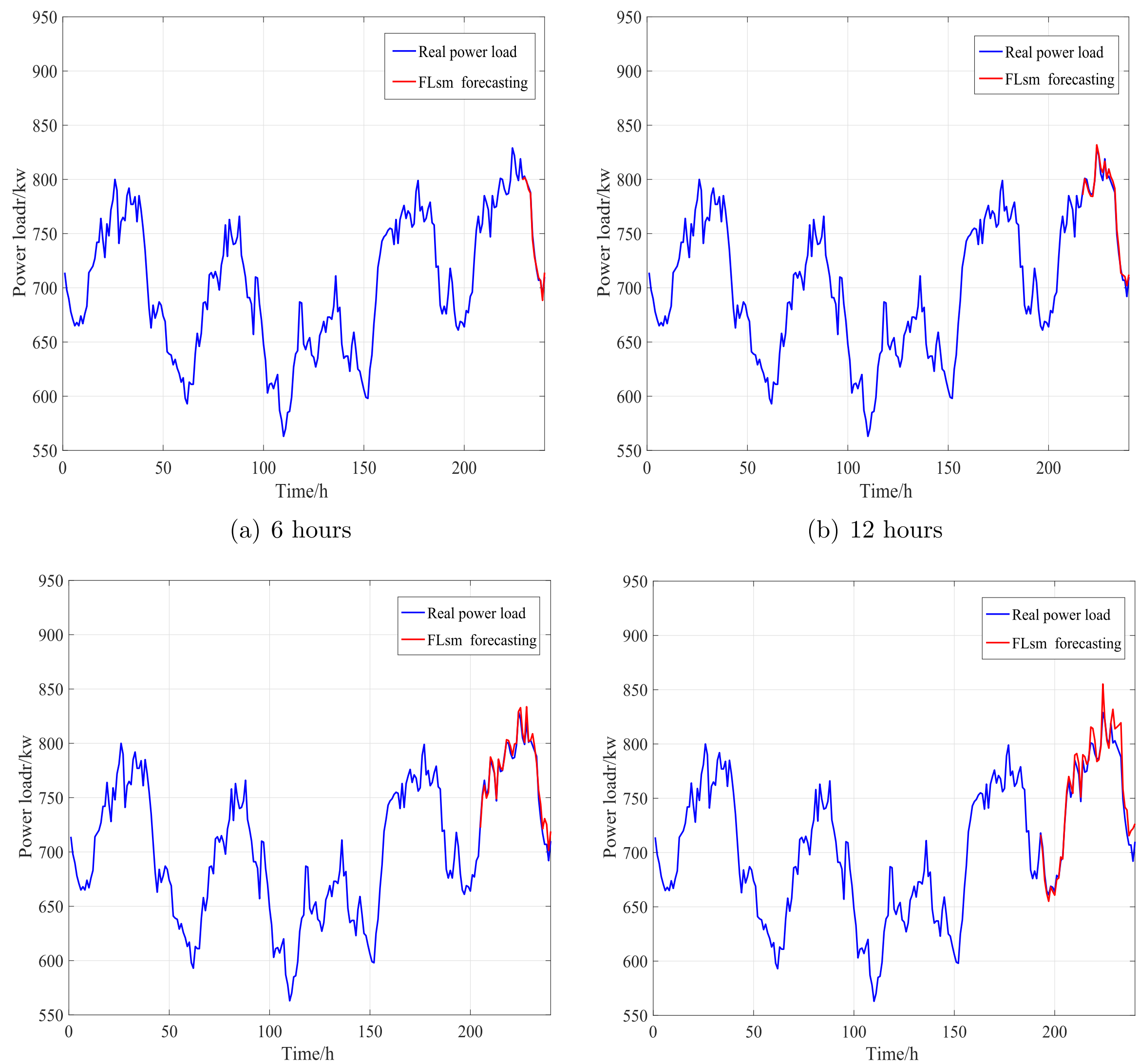

(a) 6 hours (b) 12 hours (c) 18 hours (d) 24 hours

Fig. 16. Weekend power load forecasting trend.

Table 2
The forecasting relative error (%) of power loads on adjacent dates.

	Max	Mean	Median	Stand deviation	MAPE
6 h	0.70	−0.14	−0.2	0.39	0.08
12 h	1.76	0.32	0.13	0.78	0.32
18 h	3.59	0.57	0.33	1.05	0.61
24 h	4.61	1.25	0.85	1. 52	1.49

Table 3
The forecasting relative error (%) of power loads on adjacent dates.

	Max	Mean	Median	Stand deviation	MAPE
6 h	0.86	−0.18	−0.19	0.45	0.09
12 h	1.83	0.25	0.08	0.83	0.33
18 h	3.75	0.79	0.72	1.13	0.76
24 h	4.89	1.3	0.76	1. 71	1.57

trend for the next weekend. Since the power load trends over the weekend are similar, and the power load sequence between each weekend also has LRD characteristics. Therefore, it can also be used to forecast the trend of power load. Weekend power load forecasting results and error analysis are shown in Fig. 14, Table 3 and Fig. 15, respectively.

Table 4
The forecasting relative error (%) of power loads on adjacent dates.

	Max	Mean	Median	Stand deviation	MAPE
6 h	0.59	−0.07	−0.13	0.35	0.07
12 h	1.44	0.27	0.33	0.53	0.24
18 h	3.35	0.27	0.32	0.9	0.55
24 h	3.35	0.87	0.56	1.38	1.18

4.3. Case 3: Workday and weekend

We repeated the analysis of Cases 1 and 2. In this case, to better prove the randomness of the fLsm model, we use the power load data simulation in the fourth week of October. The power load data from Wednesday to Saturday is used as historical data to forecast the power trend on Sunday. Because Wednesday to Friday are workday and Saturday is holiday, their electricity consumption is different, so it reflects the randomness of the power load and can better verify the nature of the fLsm stochastic model. Sunday power load forecasting results and error analysis are shown in Fig. 16, Table 4 and Fig. 17, respectively.

The experimental results show that the maximum error of power load trend in the next 24 h is 4.61%, 4.89% and 4.34%,

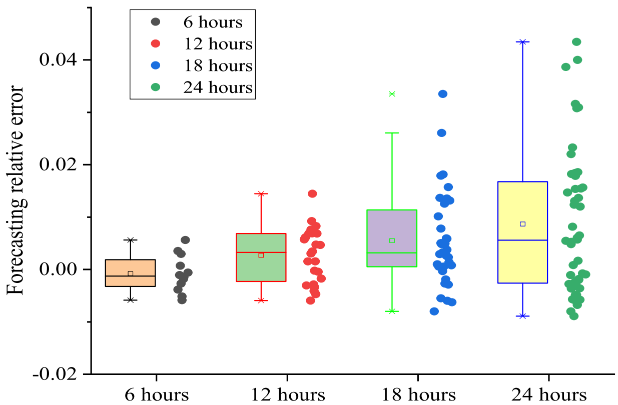

Fig. 17. Box plot analysis of relative error.

which is within the acceptable range of industry. Accurate load forecasting is the guarantee for realizing scientific of electric power dispatching scheme, which is beneficial to plan power consumption management, rational arrangement of grid operation mode and unit maintenance plan. It is not only energy-saving but also an important work to ensure reliable power supply of the grid, which has a very important impact on reducing the cost of power generation. So, it can be explained that the power load forecast based on the fLsm finite difference iterative forecasting model is effectively.

At the same time, in order to analyze the effectiveness of fLsm more comprehensively, the mean value, maximum value, median value, standard deviation and mean absolute percentage value of the errors of relative are given in these cases. The results in Tables 2–4 indicate that the relative error of the forecasting result increases if the forecasting time series increases. The forecasting results are consistent with the LRD characteristics. As the distance increases, the long correlation and the forecast effect gradually decreases. It is shown that the forecasting model of long-range dependence random sequence can be established by the fractional Lévy stable motion, and the power load time series with random characteristics can be effectively forecast. In other words, the random sequences of the process of equipment degradation, the financial markets, etc with long-range dependent characteristics can also be effectively forecast by the iterative forecasting model.

5. Conclusion

In this article, we introduced the fractional Lévy stable motion model by the form of stochastic integral and incremental process. In doing this, we analyzed the self-similarity and long-range dependent characteristics of fractional Lévy stable motion through the relationship between self-similarity parameter and the characteristic index. The discrete stochastic differential equation of fractional Lévy stable motion was obtained by the Black–Scholes model and the Maruyama notation of the fractional order. The long-range dependence finite difference iterative forecasting model was established by substituting the discretized stochastic differential equation into the difference equation. The parameters of the forecasting model are obtained by using the rescaled range analysis and the novel characteristic function method. The model was applied for forecasting of the power load time series. The accuracy of the forecasting results lies within the acceptable range for industry.

We have studied only the forecasting model, which is based on the fractional Lévy stable motion. As it is known, there exist other models, e.g., real-valued harmonic fractional Lévy processes, which can also be viewd as the generalized model of fractional Lévy motion and provides ideas for future research on stochastic sequence forecasting.

Declaration of Competing Interest

No conflict of interest exits in the submission of this manuscript, and manuscript is approved by all authors for publication. I would like to declare on behalf of my co-authors that the work described was original research that has not been published previously, and not under consideration for publication elsewhere, in whole or in part. All authors have seen the manuscript and approved to submit to your journal.

CRediT authorship contribution statement

He Liu: Methodology, Writing - original draft. **Wanqing Song:** Validation. **Ming Li:** Data curation. **Aleksey Kudreyko:** Writing - review & editing. **Enrico Zio:** Supervision.

Acknowledgments

This work was partly supported by the National Natural Science Foundation of China NSFC under grant nos. 61672238, 61272402 and the Natural Science Foundation of Shanghai under the project number 14ZR1418500.

Appendix A. Parameter estimation with the characteristic function

In the study by Xueyun Wang et al. [27,42], several parameter estimation are introduced and the validity of these methods is compared, including Quantiles method, Empirical Characteristic Function method, Logarithmic Moment method, Monte Carlo method, etc. It is concluded that the characteristic function accuracy method is better. The parameter estimation methodology can be subdivided in the following steps:

Step 1: Let $x_i|_{i=1\ldots N}$ are the sampling data for the fLsm.

Step 2: δ estimation,

$$|\varphi(\theta;\alpha,\beta,\mu,\delta)| = \left|E\{e^{j\theta x}\}\right| = e^{-\delta|\theta|^{\alpha}}, \tag{19}$$

$$\ln|\varphi(\theta;\alpha,\beta,\mu,\delta)| = -\delta|\theta|^{\alpha}, \tag{20}$$

$$\delta = -\ln|\varphi(1;\alpha,\beta,\mu,\delta)| = -\ln\left|E\{e^{jx}\}\right|. \tag{21}$$

The estimated δ has the form:

$$\hat{\delta} = -\ln|\hat{\varphi}(1;\alpha,\beta,\mu,\delta)| = -\ln\frac{1}{N}\left|\sum_{i=1}^{N}e^{jx_i}\right|. \tag{22}$$

Step 3: Further, we estimate parameter α,

$$\theta_0^{\alpha} = \frac{\ln\left|E\{e^{j\theta_0 x}\}\right|}{\ln\left|E\{e^{jx}\}\right|} = \frac{\ln|\hat{\varphi}(\theta_0;\alpha,\beta,\mu,\delta)|}{\ln|\hat{\varphi}(1;\alpha,\beta,\mu,\delta)|}, \tag{23}$$

$$\hat{\alpha} = \log_{\theta_0}\left(\frac{\ln|\hat{\varphi}(\theta_0;\alpha,\beta,\mu,\delta)|}{\ln|\hat{\varphi}(1;\alpha,\beta,\mu,\delta)|}\right), \tag{24}$$

where $\hat{\varphi}(\theta_0;\alpha,\beta,\mu,\delta) = \frac{1}{N}\left|\sum_{i=1}^{N}e^{j\theta_0 x_i}\right|$.

Step 4: Parameter μ is estimated by complex domain of the cumulant generating function of fLsm,

$$\ln\varphi(\theta_0;\alpha,\beta,\mu,\delta) = \delta|\theta|^{\alpha} + j\left[\delta|\theta|^{\alpha}\beta\frac{\theta}{|\theta|}\tan\left(\frac{\pi\alpha}{2}\right)+\mu\theta\right], \tag{25}$$

$$\hat{\mu} = \frac{\mathrm{Im}\{\theta_0^{\hat{\alpha}}\ln|\hat{\varphi}(1;\alpha,\beta,\mu,\delta)| - \ln|\hat{\varphi}(\theta_0;\alpha,\beta,\mu,\delta)|\}}{\theta_0^{\alpha}-\theta_0}. \tag{26}$$

Step 5: As we know that the fLsm model drive function is symmetric, then $\hat{\beta} = 0$.

References

[1] Xu M, Baraldi P, Al-Dahidi S, Zio E. Fault prognostics by an ensemble of echo state networks in presence of event based measurements. Eng Appl Artif Intell 2020;87:103346. doi:10.1016/j.engappai.2019.103346.

[2] Ni L-P, Ni Z-W, Gao Y-Z. Stock trend prediction based on fractal feature selection and support vector machine. Expert Syst Appl 2011;38:5569–76. doi:10.1016/j.eswa.2010.10.079.

[3] Sun K, Qiu J, Karimi HR, Gao H. A novel finite-time control for nonstrict feedback saturated nonlinear systems with tracking error constraint. IEEE Trans Syst Man Cybern 2019:1–12. doi:10.1109/TSMC.2019.2958072.

[4] Qiu J, Sun K, Wang T, Gao H. Observer-based fuzzy adaptive event-triggered control for pure-feedback nonlinear systems with prescribed performance. IEEE Trans Fuzzy Syst 2019;27(11):2152–62. doi:10.1109/TFUZZ.2019.2895560.

[5] Sun K, Mou S, Qiu J, Wang T, Gao H. Adaptive fuzzy control for nontriangular structural stochastic switched nonlinear systems with full state constraints. IEEE Trans Fuzzy Syst 2019;27(8):1587–601. doi:10.1109/TFUZZ.2018.2883374.

[6] Tsai C-C, Tseng S-T, Balakrishnan N. Optimal design for degradation tests based on gamma processes with random effects. IEEE Trans Reliab - TR 2012;61:604–13. doi:10.1109/TR.2012.2194351.

[7] Qi W, Zong G, Karimi HR. Linf control for positive delay systems with semi-Markov process and application to a communication network model. IEEE Trans Ind Electron 2019;66(3):2081–91. doi:10.1109/TIE.2018.2838113.

[8] Morf H. Sunshine and cloud cover prediction based on Markov processes. Sol Energy 2014;110:615–26. doi:10.1016/j.solener.2014.09.044.

[9] Ye Z-S, Wang Y, Tsui K-L, Pecht M. Degradation data analysis using wiener processes with measurement errors. IEEE Trans Reliab 2013;62:772â780. doi:10.1109/TR.2013.2284733.

[10] Bayraktar E, Poor HV, Rao R. Prediction and tracking of long-range-dependent sequences. Syst Control Lett 2005:1083–90. doi:10.1016/j.sysconle.2005.03.004.

[11] Lahiri S, Das U, Nordman D. Empirical likelihood for a long range dependent process subordinated to a Gaussian process. J Time Ser Anal 2019. doi:10.1111/jtsa.12465.

[12] Li M. Record length requirement of long-range dependent teletraffic. Phys A 2017;472:164–87.

[13] Sottinen T, Viitasaari L. Prediction law of fractional Brownian motion. Stat Probab Lett 2016;129. doi:10.1016/j.spl.2017.05.006.

[14] Lim S, Eab CH. Some fractional and multifractional Gaussian processes: a brief introduction. Int J Mod Phys 2014;36. doi:10.1142/S2010194515600010.

[15] Song W, Li M, Li Y, Cattani C, Chi C-H. Fractional Brownian motion: difference iterative forecasting models. Chaos Solitons Fractals 2019;123. doi:10.1016/j.chaos.2019.04.021.

[16] Song W, Li M, Liang J-K. Prediction of bearing fault using fractional Brownian motion and minimum entropy deconvolution. Entropy 2016;18:418. doi:10.3390/e18110418.

[17] Samoradnitsky G, Taqqu MS. Stable Non-Gaussian Random Processes: Stochastic Models With Infinite Variance, 1. Boca Raton, FL: USA:CRC Press; 1994.

[18] Li M. Fractal time series-a tutorial review. Math Probl Eng 2010;2010. doi:10.1155/2010/157264.

[19] Daskalaki S, Katris C. Comparing forecasting approaches for internet traffic. Expert Syst Appl 2015;42:8172–83. doi:10.1016/j.eswa.2015.06.029.

[20] Denisov S, Horsthemke W, Hanggi P. Steady-state Levy flights in a confined domain. Phys Rev E 2008;77:061112. doi:10.1103/PhysRevE.77.061112.

[21] Kutner R, Masoliver J. The continuous time random walk, still trendy: fifty-year history, state of art, and outlook. Eur Phys J B 2016;90. doi:10.1140/epjb/e2016-70578-3.

[22] Zhang Y, Shi P, Nguang S, Karimi H. Observer-based finite-time fuzzy H control for discrete-time systems with stochastic jumps and time-delays. Signal Process 2014;97:252â261. doi:10.1016/j.sigpro.2013.11.006.

[23] Lu S, Molz F, Liu H. An efficient, three-dimensional, anisotropic, fractional Brownian motion and truncated fractional Levy motion simulation algorithm based on successive random additions. Comput Geosci 2003;29:15–25. doi:10.1016/S0098-3004(02)00073-0.

[24] Nowak P, Romaniuk M. A fuzzy approach to option pricing in a Levy process setting. Int J Appl Math Comput Sci 2013;23:613–22. doi:10.2478/amcs-2013-0046.

[25] Bender C, Lindner A, Schicks M. Finite variation of fractional Levy processes. J Theor Probab 2011;25. doi:10.1007/s10959-010-0339-y.

[26] Huillet T. Fractional Levy motions and related processes. J Phys A Math Gen 1999;32:7225. doi:10.1088/0305-4470/32/42/301.

[27] Bhaskar H, Mihaylova L, Achim A. Video foreground detection based on symmetric alpha-stable mixture models. Circuits Syst Video Technol IEEE Trans 2010;20:1133–8. doi:10.1109/TCSVT.2010.2051282.

[28] Janicki A, Weron A. Can one see alpha-stable variables and processes? Stat Sci 1994;9. doi:10.1214/ss/1177010656.

[29] Hassannejad Bibalan M, Amindavar H, Amirmazlaghani M. Characteristic function based parameter estimation of skewed alpha-stable distribution: an analytical approach. Signal Process 2016;130. doi:10.1016/j.sigpro.2016.07.020.

[30] Benassi A, Cohen S, Istas J. On roughness indices for fractional fields. Bernoulli 2004;10. doi:10.3150/bj/1082380223.

[31] Benassi A, Cohen S, Istas J. Identification and properties of real harmonizable fractional Lévy motions. Bernoulli 2002;8.

[32] Marquardt T. Fractional Levy processes with an application to long memory moving average processes. Bernoulli 2006;12. doi:10.3150/bj/1165269152.

[33] Zou H-L, Yu Z, Anh V, Ma Y-L. From standard alpha-stable Levy motions to horizontal visibility networks: dependence of multifractal and laplacian spectrum. J Stat Mech 2018;2018:53403. doi:10.1088/1742-5468/aaac3d.

[34] Karasaridis A, Hatzinakos D. Network heavy traffic modeling using stable self-similar processes. Commun IEEE Trans 2001;49:1203–14. doi:10.1109/26.935161.

[35] Song WQ, Cheng XX, Cattani C, Enrico Z. Multi-fractional Brownian motion and quantum-behaved partial swarm optimization for bearing degradation forecasting. Complexity 2020;in press.

[36] Longjin L, Ren F-Y, Qiu W-Y. The application of fractional derivatives in stochastic models driven by fractional Brownian motion. Phys A 2010;389:4809–18. doi:10.1016/j.physa.2010.06.016.

[37] Ortigueira M, Batista A. On the relation between the fractional Brownian motion and the fractional derivatives. Phys Lett A 2008;372:958–68. doi:10.1016/j.physleta.2007.08.062.

[38] Yan L, Shen G, He K. Ito's formula for a sub-fractional Brownian motion. Commun Stoch Anal 2011;5:135–59. doi:10.31390/cosa.5.1.09.

[39] Scholes M, Black F. The pricing of options and corporate liabilities. J Political Econ 1973;81:637–54. doi:10.1086/260062.

[40] Wang X-T, Qiu W-Y, Ren F-Y. Option pricing of fractional version of the Black–Scholes model with hurst exponent H being in (1/3,1/2). Chaos Solitons Fractals 2001;12(3):599–608. doi:10.1016/S0960-0779(00)00028-X.

[41] Jumarie G. On the representation of fractional Brownian motion as an integral with respect to (dt)a. Appl Math Lett 2005;18(7):739–48. doi:10.1016/j.aml.2004.05.014.

[42] Wang X, Gao P, Meng S. Research on parameter estimation methods for alpha stable noise in a laser gyroscope's random error. Sensors (Basel, Switzerland) 2015;15:18550–64. doi:10.3390/s150818550.

[43] Mercik S, Weron K, Burnecki K, Weron A. Enigma of self-similarity of fractional Levy stable motions. Acta Phys Pol B 2003;34:3773.

[44] Laskin N, Lambadaris I, Harmantzis FC, Devetsikiotis M. Fractional Levy motion and its application to network traffic modeling. Comput Netw 2002;40:363–75. doi:10.1016/S1389-1286(02)00300-6.

[45] Kogon S, Manolakis S. Signal modeling with self-similar stable processes: the fractional Levy stable motion model. IEEE Trans Signal Process 1996;44:1006–10. doi:10.1109/78.492557.

[46] Li M, Zhang P, Leng J. Improving autocorrelation regression for the hurst parameter estimation of long-range dependent time series based on golden section search. Phys A 2015;445. doi:10.1016/j.physa.2015.10.071.

[47] Mandelbrot B, Wallis J. Robustness of the rescaled range R/S in the measurement of noncyclic long-run statistical dependence. Water Resour Res 1969;5:967–88. doi:10.1029/WR005i005p00967.

[48] Zanzotto PA. On solutions of one-dimensional stochastic differential equations driven by stable Levy motion. Stoch Process Their Appl 1997;68:209–28. doi:10.1016/S0304-4149(97)00030-6.

[49] Song W, Cattani C, Chi C-H. Multifractional Brownian motion and quantum-behaved particle swarm optimization for short term power load forecasting: an integrated approach. Energy 2020;194:116847. doi:10.1016/j.energy.2019.116847.

[50] Jumarie G. Merton's model of optimal portfolio in a Black–Scholes market driven by a fractional Brownian motion with short-range dependence. Insurance 2005;37:585–98. doi:10.1016/j.insmatheco.2005.06.003.

[51] W D, Heyde C. Ito's formula with respect to fractional Brownian motion and its application. J Appl Math Stoch Anal 1996;9. doi:10.1155/S104895339600038X.

[52] LemieuxMonte C. Carlo and Quasi-Monte Carlo Sampling[M]. New York: Springer; 2009. doi:10.1007/978-0-387-78165-5.

[53] Lotfi A. Application of Learning Fuzzy Inference Systems in Electricity Load Forecast. In report of the EUNITE worldwide competition on Electricity Load Forecast using Intelligent Techniques. ISBN; 2002. p. 123–30. ISBN; 80-89066-41-0.